



Published in final edited form as:

Curr Biol. 2013 November 18; 23(22): 2296–2302. doi:10.1016/j.cub.2013.09.055.

A genetic network conferring canalization to a bistable patterning system in *Drosophila*

Jackie Gavin-Smyth¹, Yu-Chiun Wang^{2,†}, Ian Butler^{1,§}, and Edwin L. Ferguson^{1,2,*}

¹Department of Molecular Genetics and Cell Biology, University of Chicago, Chicago, IL

²Department of Organismal Biology and Anatomy, University of Chicago, Chicago, IL

SUMMARY

To achieve the “constancy of the wild type,” the developing organism must be buffered against stochastic fluctuations and environmental perturbations [1]. This phenotypic buffering has been theorized to arise from a variety of genetic mechanisms [2] and is widely thought to be adaptive and essential for viability. In the *Drosophila* blastoderm embryo, staining with antibodies against the active, phosphorylated form of the Bone Morphogenetic Protein (BMP) signal transducer Mad, pMad [3, 4], or visualization of the spatial pattern of BMP-receptor interactions [5] reveals a spatially bistable pattern of BMP signaling centered on the dorsal midline. This signaling event is essential for the specification of dorsal cell fates, including the extraembryonic amnioserosa [5–7]. BMP signaling is initiated by facilitated extracellular diffusion [4, 8] that localizes BMP ligands dorsally. BMP signaling then activates an intracellular positive feedback circuit that promotes future BMP-receptor interactions [5, 6]. Here, we identify a genetic network comprising three genes that canalizes this BMP signaling event. The BMP target *eiger* (*egr*) acts in the positive feedback circuit to promote signaling, while the BMP binding protein encoded by *crossveinless-2* (*cv-2*) antagonizes signaling. Expression of both genes requires the early activity of the homeobox gene *zerknüllt* (*zen*). Two *Drosophila* species lacking early *zen* expression have high variability in BMP signaling. These data both detail a new mechanism that generates developmental canalization and identify an example of a species with non-canalized axial patterning.

RESULTS

We developed techniques to quantify pMad staining in individual embryos at the onset of gastrulation (Stage 6) and compare intensities among wild-type embryos and between wild-type embryos and embryos of a second genotype (Supplemental experimental procedures and Figures S1A–S1C). pMad staining in wild-type embryos, measured in a 60 micron region centered at 50% egg length, first appears in a low intensity, broad domain in the Stage 5 mid-cellularization embryo. By Stage 6, 30 minutes later, pMad staining intensifies

*Correspondence to: elfergus@uchicago.edu.

†Current address: Department of Molecular Biology, Princeton University, Princeton, NJ.

§Current address: Laboratory of Insect Social Evolution, Rockefeller University, New York, NY.

Publisher's Disclaimer: This is a PDF file of an unedited manuscript that has been accepted for publication. As a service to our customers we are providing this early version of the manuscript. The manuscript will undergo copyediting, typesetting, and review of the resulting proof before it is published in its final citable form. Please note that during the production process errors may be discovered which could affect the content, and all legal disclaimers that apply to the journal pertain.

and refines to a sharp stripe (Figures 1A and 1B) [3–5]. In wild-type embryos, the spatial extent of pMad staining is highly invariant (Figure 1C). The mean half-maximal width of the pMad domain, an approximate measure of the steepness of the BMP gradient, is 23.8 microns, SEM 0.98 microns (Figure 1D). The coefficient of variance (σ/μ) of pMad intensity at each Dorsal/Ventral (D/V) position is below 0.3 (Figure 1E). These data are in agreement with previous findings [7] and demonstrate the uniformity of BMP signaling in wild-type *D. melanogaster* embryos during dorsal patterning. Posterior to the cephalic furrow, cells with BMP signaling above a given level (see below) are fated to become extraembryonic amnioserosa. Amnioserosa cells no longer divide, but instead undergo cycles of endoreduplication to become a polyploid squamous epithelium. Similar to the spatial uniformity of the BMP signaling domain, the variability of amnioserosa cell numbers in wild-type embryos is very low ($\sigma/\mu = 0.07$). We then sought to identify genes that canalize the width and intensity of the BMP signaling domain and subsequent cell fate specification.

The *eiger*/JNK pathway promotes BMP signaling

BMP transcriptional activity is required for formation of the wild-type BMP signaling domain, as Stage 6 embryos derived from germline clones of a null allele of *Medea*, an obligate BMP transcriptional cofactor, manifest a broad pattern of receptor ligand interactions [5] and an expanded, low intensity pMad domain (Figures 1F and 1G) with a mean half-maximal width of 73.6 microns, SEM 11.7 microns. The expansion of the pMad domain in *Medea* mutant embryos indicates that one or more BMP target genes are required for the spatial restriction of BMP signaling.

The *Drosophila* Tumor Necrosis Factor- α homolog *egr* [9] has a dynamic dorsal expression pattern [10] consistent with a BMP target gene: initially, *egr* is broadly expressed in the dorsal region of Stage 5 embryos, but is restricted to the dorsal most cells in Stage 6 embryos (Figures 2A and 2B). *egr* transcription and protein expression in the pregastrula embryo is dependent on BMP signaling, as both are greatly reduced in a *dpp* null embryo and *egr* transcription is restored by local expression of *dpp* (Figures 2C–2F). Egr is an activator of the Jun N-terminal kinase (JNK) pathway, and its activity in two biological contexts is dependent on the JNK homolog *basket* (*bsk*) [9, 11]. The mean intensity of pMad staining in *egr* null embryos, or embryos in which maternal *bsk* activity was disrupted by germline-specific expression of *bsk* RNAi (*bsk* RNAi embryos), is half that of wild-type embryos (Figures 3A and 3B, S2A and S2B) with minimal variation in pMad intensity (Figure 3C). However, *egr* embryos have a significantly expanded mean half-maximal width of pMad staining of 39 microns, SEM 1.4 microns (Figure S2I), indicating a shallowly graded BMP signaling domain. Taken together with the previous findings showing Egr acts cell autonomously [11, 12], these data indicate *egr* is a locally acting component of the positive feedback circuit necessary for the intensification and refinement of BMP signaling.

Despite decreased intensity of BMP signaling, both *egr* and *bsk* RNAi embryos specify amnioserosa cells in numbers very similar to, or only slightly less than, the wild type (Figures 3M, S2O and see Supplemental experimental procedures for comparison statistics), indicating that the level of BMP signaling in wild type is at least double that necessary to specify the amnioserosa cell fate. The loss of *egr*/JNK activity can be enhanced by a partial

reduction in BMP signal transduction, resulting both in a spatial expansion of low levels of pMad staining, due to a loss of refinement of the signaling domain, and in decreased amnioserosa cell numbers, due to reduction in the efficacy of BMP signaling (Figures S2D–S2O). Therefore, while *egr* and JNK activity contribute significantly to wild-type BMP signaling, additional BMP target genes likely contribute to the positive feedback circuit.

***cv-2* antagonizes BMP signaling**

We also examined the effect of another dorsally-expressed gene, *cv-2*, on BMP signaling in the early embryo. *cv-2* encodes a cell-surface BMP binding protein, that can either antagonize or promote BMP signaling in a dosage and context dependent manner [13, 14]. At high concentrations, relative to BMP receptors, Cv-2 can act as an antagonist, whereas at lower concentrations it has a positive effect on BMP signaling. Modeling suggests this duality of Cv-2 allows it to function either as an antagonist ligand sink or an agonistic ligand source [14]. Zygotic *cv-2* is initially expressed in a *dpp*-independent pattern in the dorsal 40% of the Stage 5 embryo [14, 15] (Figures 2I and 2K), indicating *cv-2* is not a component of the BMP transcriptional feedback circuit. At Stage 6, a distinct, *dpp* dependent expression of *cv-2* appears in the amnioserosa anlage (arrowhead, Figure 2J).

cv-2 embryos from *cv-2* females have a mean peak pMad intensity approximately double that of wild type (Figures 3D and 3E). pMad intensity in *cv-2* embryos has low variability in peak regions but moderate variability in lateral regions, indicative of a variable expansion of the signaling domain (Figure 3F). Although *in situ* analysis indicates there are no uniformly distributed maternal *cv-2* transcripts in the stage 5 embryo [14] (Figure 2I), *cv-2* is transcribed in ovarioles (Figure S3A), and gene dosage experiments indicated that both maternal and zygotic *cv-2* activities contribute to the *cv-2* phenotype (Figures S3B–S3I). While there is evidence, presented below, that Cv-2 can also act as a BMP agonist, the increased pMad intensity in the absence of all *cv-2* activity indicates that Cv-2 acts primarily as a potent antagonist of BMP signaling in the early embryo.

BMP signaling is decanalized in the absence of *egr* and *cv-2*

To characterize the effect of loss of both positive and negative modulators of BMP signaling, we examined the phenotype of *egr cv-2* double mutant embryos. While the mean intensity of pMad signaling in the double mutant embryos is similar to that observed in wild type (Figures 3G and 3H), the variability of BMP signaling is extremely high (Figures 3I and 3N). Specifically, the variability of peak intensity in *egr cv-2* embryos is significantly different from wild type or either single mutant (see Supplemental experimental procedures for full comparison statistics). The variability in BMP signaling in *egr cv-2* embryos correlates with a significantly increased variability of amnioserosa cell number (Figure 3M). Thus, while the activity of either *egr* or *cv-2* is sufficient to ensure the invariance of BMP signaling, the loss of the activities of both genes results in decanalized BMP signaling and amnioserosa specification during D/V patterning.

As developmental canalization has been proposed to buffer against environmental and/or genetic variation [1], we wished to determine whether *egr cv-2* embryos were more susceptible to either perturbation. The variability in pMad intensity and amnioserosa

specification in *egr cv-2* embryos raised at 25°C (Figures 3I, 3M and 3N) is not further increased by incubation at either higher (29°C) or lower (18°C) temperatures (Figures S4A–S4D and S4H). In contrast, maternal heterozygosity for *Med13* in *egr cv-2* embryos leads to a decrease in the average number of amnioserosa cells and a marked increase in the variability of amnioserosa cell number (Figure S4H), despite an average pMad intensity equivalent to wild-type embryos (Figures S4E and S4F), and a variability equivalent to that of *egr cv-2* embryos (compare Figure 3I to Figure S4G). The increased rate of catastrophe, or failure to specify any amnioserosa cells, in *egr cv-2* embryos carrying an otherwise subliminal *Medea* mutation (Figures S2D–S2F and S2O) demonstrates that without the activities of *egr* and *cv-2*, embryos are highly susceptible to minor genetic perturbations in BMP signal transduction. These data suggest that the combined action of *egr* and *cv-2* buffers the embryo against intrinsic or genetic fluctuations resulting in changes in the efficacy of BMP signaling.

Pre-gastrula *zen* is necessary for *egr* and *cv-2* transcription

Previous work demonstrated that activity of the homeobox gene *zen* affects Dpp-receptor interactions prior to gastrulation [5]. *zen* is initially expressed in a BMP-independent manner in the dorsal 40% of the blastoderm embryo (Figure 4A) [16, 17]; however, no function has been attributed to this pre-gastrula *zen* expression. In contrast, the subsequent BMP-dependent *zen* expression [18] (Figure 4B) in the amnioserosa anlage at the onset of gastrulation has been well documented as necessary for amnioserosa specification [19–21]. We found that stage 5 *zen* mutant embryos lack transcription of both *egr* and *cv-2* (Figures 2G, 2H, and 2L). Furthermore, the variability of BMP signaling in *zen* mutant embryos is much higher than that observed in wild-type embryos (Figure 3L), consistent with its role in controlling the transcription of both *egr* and *cv-2*. Thus, *zen* and its downstream targets, *egr* and *cv-2*, define a genetic network that confers robustness to BMP signaling during dorsal patterning (Figure 2M).

zen mutants have elevated BMP signaling

zen mutant embryos also show both a doubling of pMad intensity and a spatial expansion of signaling as compared to wild-type embryos or *egr cv-2* embryos from homozygous mothers (Figures 3J and 3K). While *zen* mutant embryos lack zygotic expression of *egr* and *cv-2*, they retain a maternal contribution of Cv-2 protein. The observed increase in pMad intensity in *zen* embryos is likely due to an agonistic action of maternal Cv-2 protein. We found that BMP signaling in *egr cv-2* embryos from heterozygous mothers display elevated BMP signaling compared to *egr cv-2* embryos from homozygous mothers (compare Figures S3J and S3K to Figures 3G and 3H). Thus, low levels of maternal Cv-2 protein can elevate BMP signaling in the absence of *egr*.

To confirm the effect of pregastrula *zen* activity while circumventing the absolute requirement for later *zen* in the specification of amnioserosa, we overexpressed *egr* or an active form of the JNKK *hemipterous* in a *zen/+* background. While embryos of each of the three single genotypes had wild-type levels of BMP signaling and amnioserosa specification (Figures S5A–S5F and Table S1), the overexpression of these two constructs in *zen/+* embryos caused an increase in pMad intensity and breadth, as well as in the number of

amnioserosa cells (Figures S5G–S5J and Table S1). Thus, the pregastrula activity of *zen* reduces BMP signaling. Notably, however, uniform expression of an activated form of the *Jun* homolog, *Jra* [22], in *zen/+* embryos did not expand signaling or increase amnioserosa specification (Figures S5K and S5L and Table S1), suggesting that the interaction of the JNK and BMP signaling pathways is not dependent on *Jra*-mediated transcription, but rather involves direct phosphorylation of one or more proteins by the JNK Basket.

Drosophila species with non-canalized BMP signaling during D/V patterning

The blastoderm expression of *zen* in *D. melanogaster* is controlled by the conserved Ventral-Repression Element (VRE) 1.6kb upstream of the *zen* coding region. The VRE contains activating TAGteam binding sites [23] for the zinc-finger transcription factor Zelda [24] (Figure S6E). To determine whether early *zen* expression, and the consequent canalization of embryonic D/V patterning, is also conserved throughout the *Drosophila* lineage (Figure S6A), we first examined the TAGteam sites upstream of the *zen* gene in other species. The closely related species *D. simulans* has four conserved TAGteam sites (Figure S6F) and displays very low variability in BMP signaling (Figure S6B). Two other *Drosophila* species, *D. yakuba* and *D. santomea*, have non-conservative changes in the TAGteam sites (Figure S6F). *D. yakuba* is found throughout sub-Saharan Africa, while its sister species *D. santomea* is endemic to the island of São Tomé [25–27]. Consistent with the changes in TAGteam sequences, the only detectable *zen* expression in early Stage 5 embryos of *D. yakuba* and *D. santomea* is a faint anterior dorsal band (Figures 4C and 4E). As a likely consequence, Stage 5 embryos of both species have greatly reduced *Egr* expression (Figures 4I and 4K) compared to *D. melanogaster* (Figure 4G). In contrast, in Stage 6 embryos of all three species, *zen* and *Egr* expression are similar (Figures 4H, 4J, and 4L). Therefore, alteration of the canonical TAGteam sites in the VRE correlates with the absence of early *zen* and *Egr* in *D. yakuba* and *D. santomea*.

To determine whether the loss of early *zen* expression leads to loss of phenotypic canalization of BMP signaling in these species, we examined pMad-stained Stage 6 embryos of both *D. yakuba* and *D. santomea*. pMad intensity in both species is extremely variable throughout the signaling domain with the variability of peak pMad intensity significantly greater than *D. melanogaster*, indicative of decanalized BMP signaling (Figures 4M–4R, S6C, and S6D). However, only *D. santomea* embryos have a high variability in amnioserosa cell numbers, while the variability of amnioserosa numbers in *D. yakuba* embryos is equivalent to that of *D. melanogaster* (Figure 4V). This indicates *D. yakuba* amnioserosa specification is robust to variable BMP signaling input.

The variability in *D. santomea* amnioserosa specification is not altered by temperature conditions (Table S2); however, the BMP signaling phenotype and amnioserosa specification in one wild-caught *D. santomea* isofemale line (Line 2) supports the hypothesis that the *egr cv-2* network buffers against genetic variation. As in the synthetic *D. santomea* line, this isofemale line has high variability of pMad intensity (Figures 4S and 4T). However, unlike the synthetic line, this isofemale line produced an appreciable (~10%) number of embryos that completely lacked amnioserosa (Figures 4U and 4V). The susceptibility to a naturally occurring genetic variant seen in this isofemale line illustrates

the fragility of this patterning system in the absence of a canalizing mechanism. While is unlikely that the causative genetic variant remains in the wild population, the existence of this line, however transient, demonstrates that, in the absence of the stabilizing *egr cv-2* activity in *D. santomea*, deleterious mutations have much stronger phenotypic penetrance. Therefore, as a decanalized species, *D. santomea* is rendered more vulnerable to genetic variation.

DISCUSSION

We have identified a genetic network that acts as a phenotypic stabilizer [28] of a spatially bistable patterning process. The minimal bistable systems allowed by theory require a non-linear activation rate and a linear degradation rate [29]. We believe the network we defined represents the minimal genetic components required for bistability of BMP signaling in *D. melanogaster*. In turn, bistability canalizes dorsal patterning. During amnioserosa specification, *egr* provides positive feedback, conferring non-linearity, while *cv-2* acts as a linear negative regulator of the signaling pathway. The loss of both components reveals the inherent noise of facilitated extracellular diffusion of BMP ligands, as, without *egr* and *cv-2*, embryos manifest a huge range of signaling domain breadth and intensity.

Our data also reveal that amnioserosa specification in *D. melanogaster* is robust on multiple levels, with different mechanisms ensuring robustness in various *Drosophila* species. First, *egr* or *bsk* RNAi embryos have normal amounts of amnioserosa and minimal embryonic lethality despite the two-fold reduction in signaling intensity. This demonstrates that amnioserosa specification is robust to decreases of BMP signaling and the wild type level of BMP signaling in *D. melanogaster* is much higher than that necessary. Second, the *D. melanogaster* embryo can tolerate at least a 250% increase [30] or a 20% decrease (Figure 3M) in amnioserosa cell number without compromising viability. Lastly, the variability in amnioserosa cell number in *D. yakuba* embryos is equivalent to that in *D. melanogaster* embryos, indicating that amnioserosa specification in *D. yakuba* is robust against variable BMP signaling intensity. Therefore, in *D. yakuba* embryos, either less BMP signaling is required to direct amnioserosa specification, or a second mechanism downstream of BMP signaling intensity maintains robust amnioserosa specification.

Finally, as a counterpoint to the predicted ubiquity and selective maintenance of developmental canalization [31], we have identified *D. santomea* as a non-canalized wild-type species. *D. santomea* has both highly variable cell fate specification and is not robust to genetic variants found in its wild population. The identification of this non-canalized species may permit further investigation of the evolutionary factors allowing for this diversity in developmental trajectories.

Supplementary Material

Refer to Web version on PubMed Central for supplementary material.

Acknowledgments

We thank R. Fehon, S. Horne-Badovinac, M. Kreitman, C. Li, D. Matute, J. Reinitz, M. Rust and U. Schmidt-Ott for insightful comments on the manuscript, and S. Lemke and D. Umulis for helpful discussions and encouragement. We thank Drs. M. Frasch, T. Jessell, E. Laufer, D. Matute, M. Miura, and M. O'Connor for fly stocks and reagents. This work was supported by grants from the National Institutes of Health (5R01GM050838 and 1R01GM078481).

References

1. Waddington CH. Canalization of Development and the Inheritance of Acquired Characters. *Nature*. 1942; 150:563–565.
2. Kitano H. Biological robustness. *Nat Rev Genet*. 2004; 5:826–837. [PubMed: 15520792]
3. Dorfman R, Shilo BZ. Biphasic activation of the BMP pathway patterns the *Drosophila* embryonic dorsal region. *Development*. 2001; 128:965–972. [PubMed: 11222150]
4. Shimmi O, Umulis D, Othmer H, O'Connor MB. Facilitated transport of a Dpp/Scw heterodimer by Sog/Tsg leads to robust patterning of the *Drosophila* blastoderm embryo. *Cell*. 2005; 120:873–886. [PubMed: 15797386]
5. Wang YC, Ferguson EL. Spatial bistability of Dpp-receptor interactions during *Drosophila* dorsal-ventral patterning. *Nature*. 2005; 434:229–234. [PubMed: 15759004]
6. Umulis DM, Serpe M, O'Connor MB, Othmer HG. Robust, bistable patterning of the dorsal surface of the *Drosophila* embryo. *Proc Natl Acad Sci U S A*. 2006; 103:11613–11618. [PubMed: 16864795]
7. Umulis DM, Shimmi O, O'Connor MB, Othmer HG. Organism-scale modeling of early *Drosophila* patterning via bone morphogenetic proteins. *Dev Cell*. 2010; 18:260–274. [PubMed: 20159596]
8. Ashe HL, Levine M. Local inhibition and long-range enhancement of Dpp signal transduction by Sog. *Nature*. 1999; 398:427–431. [PubMed: 10201373]
9. Igaki T, Kanda H, Yamamoto-Goto Y, Kanuka H, Kuranaga E, Aigaki T, Miura M. Eiger, a TNF superfamily ligand that triggers the *Drosophila* JNK pathway. *EMBO J*. 2002; 21:3009–3018. [PubMed: 12065414]
10. Stathopoulos A, Van Drenth M, Erives A, Markstein M, Levine M. Whole-genome analysis of dorsal-ventral patterning in the *Drosophila* embryo. *Cell*. 2002; 111:687–701. [PubMed: 12464180]
11. Igaki T, Pastor-Pareja JC, Aonuma H, Miura M, Xu T. Intrinsic tumor suppression and epithelial maintenance by endocytic activation of Eiger/TNF signaling in *Drosophila*. *Dev Cell*. 2009; 16:458–465. [PubMed: 19289090]
12. Narasimamurthy R, Geuking P, Ingold K, Willen L, Schneider P, Basler K. Structure-function analysis of Eiger, the *Drosophila* TNF homolog. *Cell Res*. 2009; 19:392–394. [PubMed: 19223855]
13. Conley CA, Silburn R, Singer MA, Ralston A, Rohwer-Nutter D, Olson DJ, Gelbart W, Blair SS. Crossveinless 2 contains cysteine-rich domains and is required for high levels of BMP-like activity during the formation of the cross veins in *Drosophila*. *Development*. 2000; 127:3947–3959. [PubMed: 10952893]
14. Serpe M, Umulis D, Ralston A, Chen J, Olson DJ, Avanesov A, Othmer H, O'Connor MB, Blair SS. The BMP-binding protein Crossveinless 2 is a short-range, concentration-dependent, biphasic modulator of BMP signaling in *Drosophila*. *Dev Cell*. 2008; 14:940–953. [PubMed: 18539121]
15. Biemar F, Nix DA, Piel J, Peterson B, Ronshaugen M, Sementchenko V, Bell I, Manak JR, Levine MS. Comprehensive identification of *Drosophila* dorsal-ventral patterning genes using a whole-genome tiling array. *Proc Natl Acad Sci U S A*. 2006; 103:12763–12768. [PubMed: 16908844]
16. Doyle HJ, Harding K, Hoey T, Levine M. Transcripts encoded by a homoeo box gene are restricted to dorsal tissues of *Drosophila* embryos. *Nature*. 1986; 323:76–79. [PubMed: 3755802]
17. Rushlow C, Frasch M, Doyle H, Levine M. Maternal regulation of *zerknüllt*: a homoeobox gene controlling differentiation of dorsal tissues in *Drosophila*. *Nature*. 1987; 330:583–586. [PubMed: 2891036]

18. Xu M, Kirov N, Rushlow C. Peak levels of BMP in the *Drosophila* embryo control target genes by a feed-forward mechanism. *Development*. 2005; 132:1637–1647. [PubMed: 15728670]
19. Hamaguchi T, Yabe S, Uchiyama H, Murakami R. *Drosophila* Tbx6-related gene, Dorsocross, mediates high levels of Dpp and Scw signal required for the development of amnioserosa and wing disc primordium. *Dev Biol*. 2004; 265:355–368. [PubMed: 14732398]
20. Reim I, Lee HH, Frasch M. The T-box-encoding Dorsocross genes function in amnioserosa development and the patterning of the dorsolateral germ band downstream of Dpp. *Development*. 2003; 130:3187–3204. [PubMed: 12783790]
21. Reim I, Mohler JP, Frasch M. Tbx20-related genes, mid and H15, are required for tinman expression, proper patterning, and normal differentiation of cardioblasts in *Drosophila*. *Mech Dev*. 2005; 122:1056–1069. [PubMed: 15922573]
22. Treier M, Bohmann D, Mlodzik M. JUN cooperates with the ETS domain protein pointed to induce photoreceptor R7 fate in the *Drosophila* eye. *Cell*. 1995; 83:753–760. [PubMed: 8521492]
23. ten Bosch JR, Benavides JA, Cline TW. The TAGteam DNA motif controls the timing of *Drosophila* pre-blastoderm transcription. *Development*. 2006; 133:1967–1977. [PubMed: 16624855]
24. Liang HL, Nien CY, Liu HY, Metzstein MM, Kirov N, Rushlow C. The zinc-finger protein Zelda is a key activator of the early zygotic genome in *Drosophila*. *Nature*. 2008; 456:400–403. [PubMed: 18931655]
25. Matute DR, Novak CJ, Coyne JA. Temperature-based extrinsic reproductive isolation in two species of *Drosophila*. *Evolution*. 2009; 63:595–612. [PubMed: 19087181]
26. Lachaise D, Harry M, Solignac M, Lemeunier F, Benassi V, Cariou ML. Evolutionary novelties in islands: *Drosophila santomea*, a new melanogaster sister species from Sao Tome. *Proc Biol Sci*. 2000; 267:1487–1495. [PubMed: 11007323]
27. Cariou ML, Silvain JF, Daubin V, Da Lage JL, Lachaise D. Divergence between *Drosophila santomea* and allopatric or sympatric populations of *D. yakuba* using paralogous amylase genes and migration scenarios along the Cameroon volcanic line. *Mol Ecol*. 2001; 10:649–660. [PubMed: 11298976]
28. Masek J, Siegal ML. Robustness: mechanisms and consequences. *Trends Genet*. 2009; 25:395–403. [PubMed: 19717203]
29. Ferrell JE, Xiong W. Bistability in cell signaling: How to make continuous processes discontinuous, and reversible processes irreversible. *Chaos*. 2001; 11:227–236. [PubMed: 12779456]
30. Wharton KA, Ray RP, Gelbart WM. An activity gradient of decapentaplegic is necessary for the specification of dorsal pattern elements in the *Drosophila* embryo. *Development*. 1993; 117:807–822. [PubMed: 8330541]
31. Meiklejohn CD, Hartl DL. A single mode of canalization. *Trends in Ecology & Evolution*. 2002; 17:468–473.

Highlights

- The BMP target gene *egr* activates the JNK pathway to promote BMP signaling.
- The BMP binding protein *Cv-2* negatively regulates BMP signaling.
- *egr* and *cv-2* expression requires pregastrula *zen*; their combined loss decanalizes BMP signaling.
- Two *Drosophila* species lack pregastrula *zen* expression and have decanalized BMP signaling.

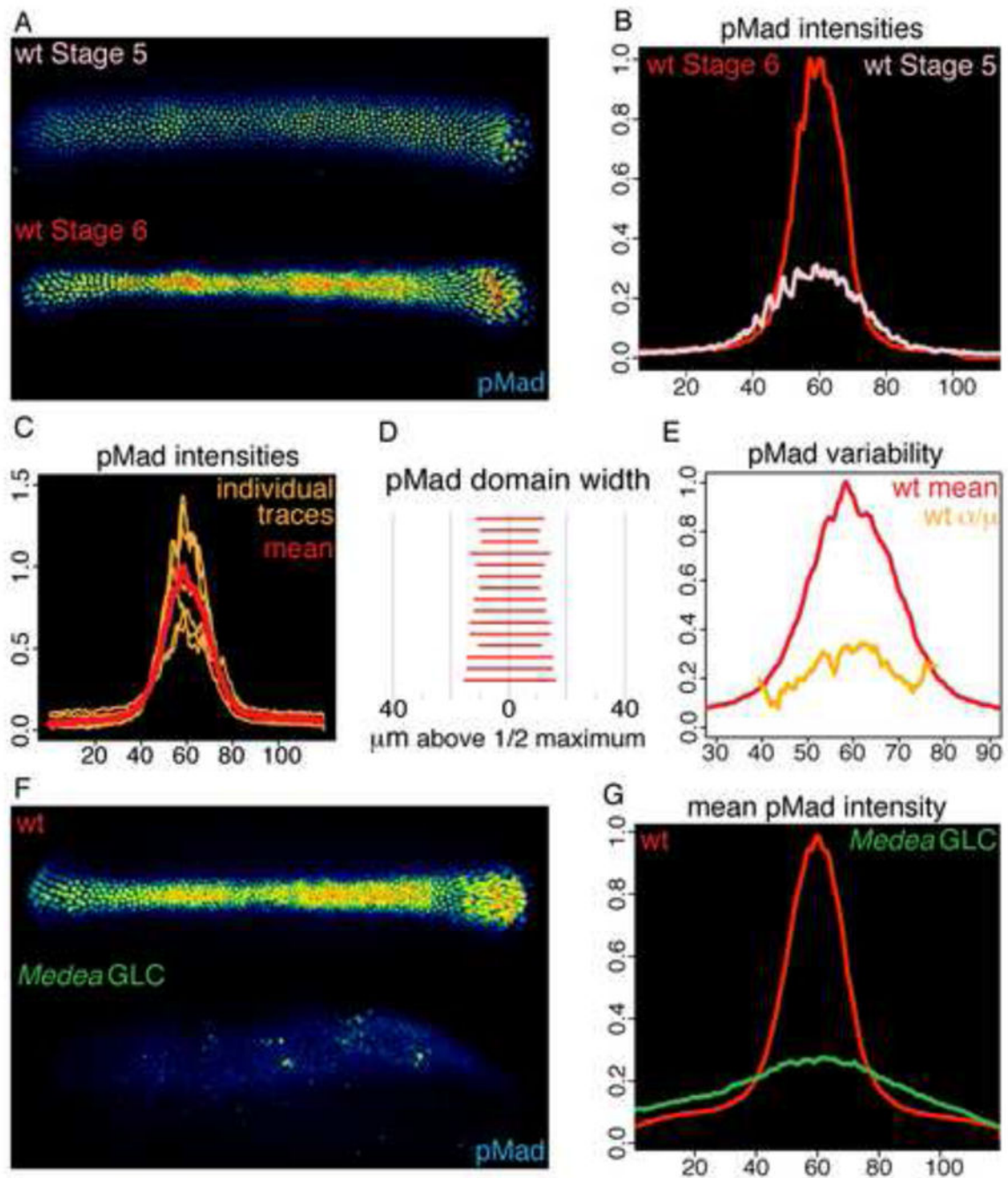


FIGURE 1. BMP signaling in wild-type and *Medea* germ line clone embryos

(A–B) Dorsal views of heat mapped pMad staining (A) and mean intensity (B) of a Stage 5 and Stage 6 wild-type embryo. All other panels with pMad staining are of Stage 6 embryos. (C) pMad intensities of individual wild-type embryos and mean intensity plotted across 120 microns of the D/V axis. (D) Width in microns of region of wild-type embryos where pMad intensity is greater than 50% of peak intensity. (E) Variability (σ/μ) of pMad staining in the population of (C) along the D/V axis. (F–G) Representative pMad staining (F) and mean

intensities (G) of 6 wild-type and 13 *Med* germ line clone embryos. See Figure S1 for related data.

Author Manuscript

Author Manuscript

Author Manuscript

Author Manuscript

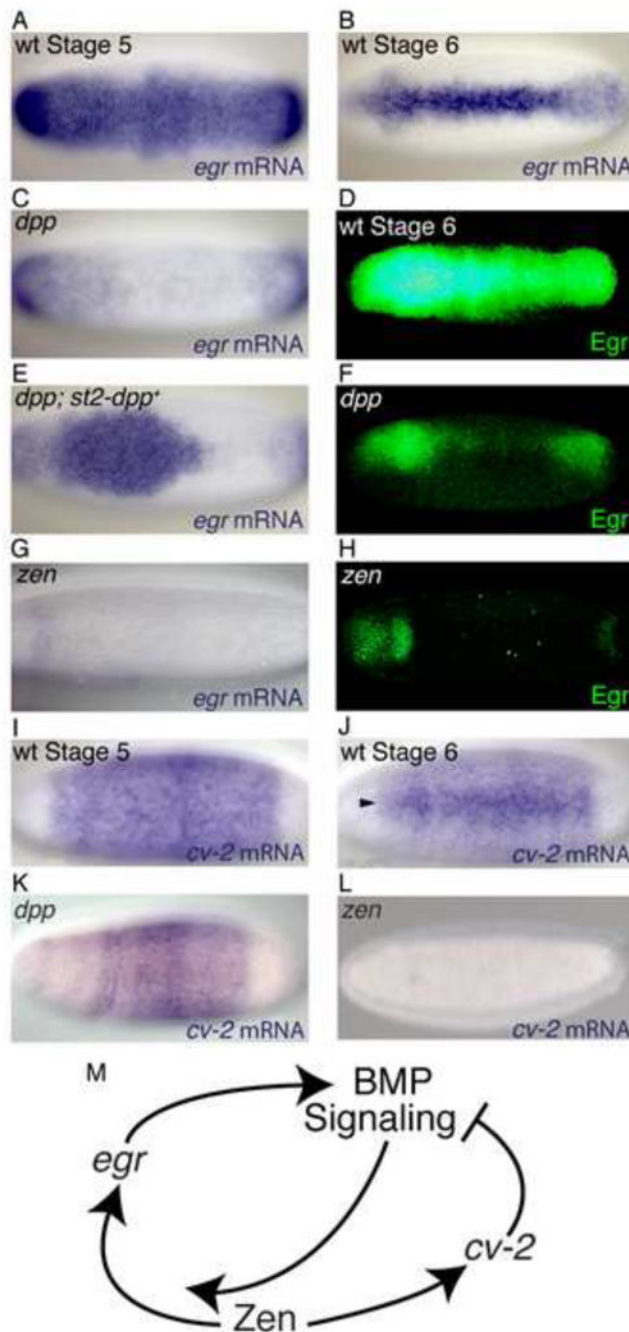


FIGURE 2. *egr* and *cv-2* expression

Dorsal views of *in situ* of *egr* mRNA in Stage 5 (A) and Stage 6 (B) wild-type embryos, Stage 6 *dpp*^{H46} (C) and *zen*⁷ (G) embryos and in a Stage 6 *dpp*^{H46} embryo carrying two copies of the *P{dpp.eve.st2}* transgene (E). Dorsal views of heat mapped Egr protein expression in Stage 6 wild-type (D), *dpp*^{H46} (F) and *zen*⁷ (H) embryos. (I–L) *in situ* of *cv-2* mRNA in Stage 5 (I) and Stage 6 (J) wild-type embryos and in Stage 5 *dpp*^{H46} (K) and *zen*⁷ (L) embryos.

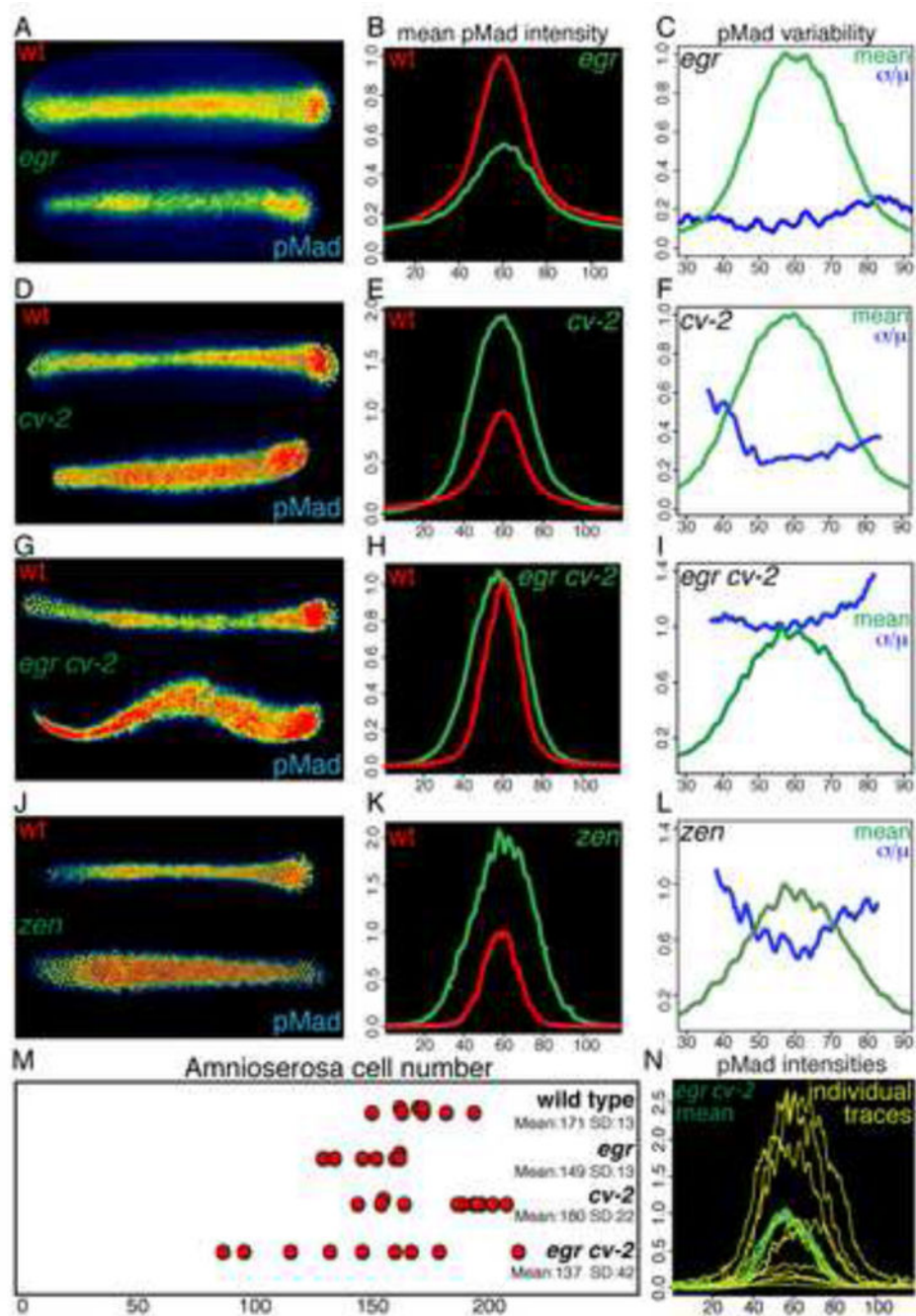


FIGURE 3. BMP signaling in *egr*, *cv-2*, *egr cv-2* and *zen* embryos
 (A–L) Representative pMad staining (A,D,G,J), mean intensities (B,E,H,K) and variability (C,F,I,L) of 6 wild-type and 9 *egr* embryos (A–C), 8 wild-type and 8 *cv-2* embryos (D–F), 7 wild-type and 15 *egr cv-2* embryos (G–I), 9 wild-type and 10 *zen*⁷ embryos (J–L). (M) Distribution, mean and standard deviation of amnioserosa cell number in wild-type, *egr*, *cv-2*, and *egr cv-2* embryos. (N) Individual traces of pMad intensities of *egr cv-2* embryos with mean intensity (light green). See Figures S2–S5 and Table S1 for related data.

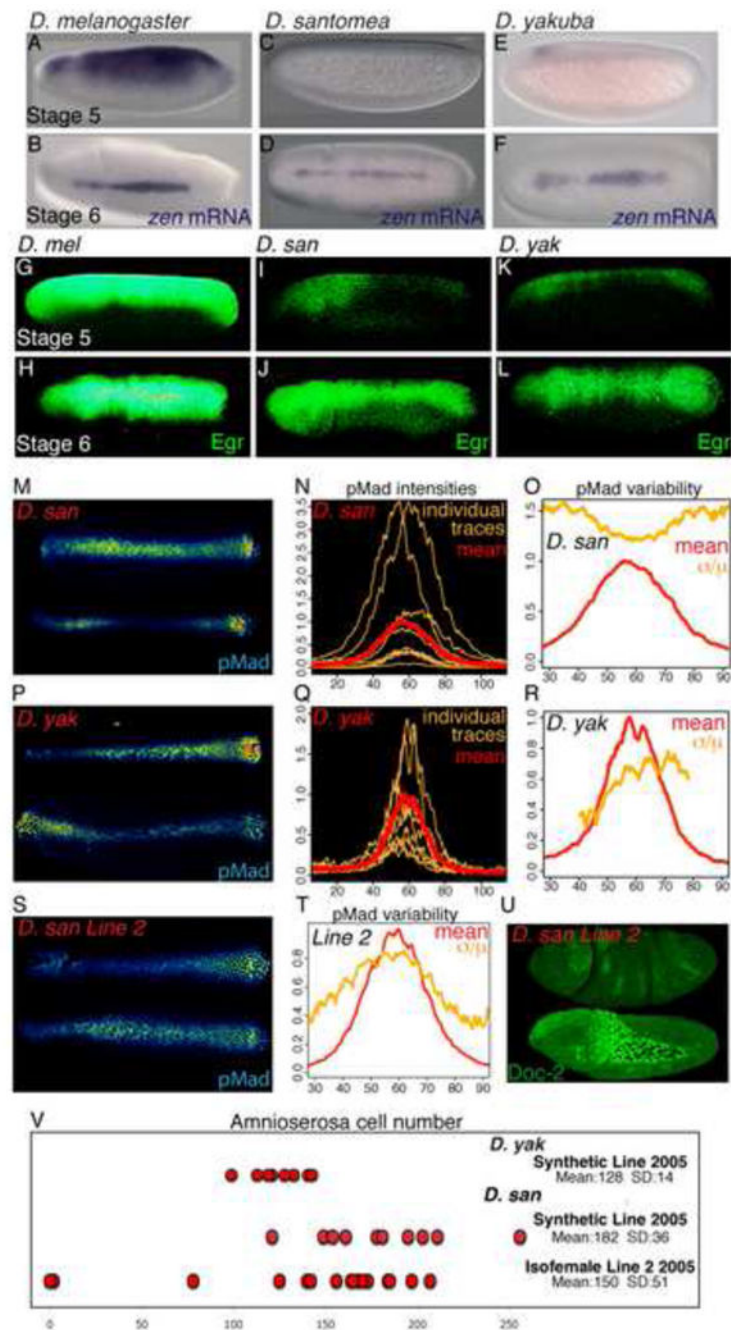


FIGURE 4. BMP signaling is variable in *D. santomea* and *D. yakuba* embryos (A–L) *in situ* of *zen* mRNA (A–F) or anti-Egr (G–L) staining in *D. melanogaster* (A–B, G–H), *D. santomea* (C–D, I–J) and *D. yakuba* embryos (E–F, K–L). Stage 5 embryos, lateral view (A, C, E, G, I, K); Stage 6 embryos, dorsal view (B, D, F, H, J, L). Representative pMad staining (M, P, S), individual and mean traces (N, Q) of pMad intensity and variability (O, R, T) of 10 *D. santomea* (M–O), 12 *D. yakuba* embryos (P–R) and 13 *D. santomea* Isofemale Line 2 embryos (S, T). (U) Lateral views of *D. santomea* Isofemale Line 2 embryos stained with anti-Dorsocross2 to identify amnioserosa cells. The top embryo

completely lacks any amnioserosa, while the bottom embryo has a normal number of amnioserosa cells. (V) Distribution, mean and standard deviation of amnioserosa cell number in *D. yakuba* and *D. santomea* Synthetic 2005 lines, and *D. santomea* Isofemale line 22005 embryos. See Figure S6 and Table S2 for related data.

Author Manuscript

Author Manuscript

Author Manuscript

Author Manuscript